Phenomenological revisit of the $B \to \pi\pi$ decays by incorporating soft color-octet contributions

Yueling Yang, Bingbing Yang, and Junfeng Sun*

School of Physics, Henan Normal University, Xinxiang 453007, China

(Received 3 September 2026; accepted 23 October 2026; published 9 November 2026)

Motivated by the long-standing "$\pi\pi$ puzzle" in nonleptonic B decays, we revisit the $B \to \pi\pi$ decays within the QCD factorization (QCDF) framework, now incorporating the soft color-octet matrix element (COME) contributions, an ingredient that has been largely overlooked in earlier QCDF studies. A comprehensive phenomenological analysis is performed under three distinct scenarios, with the free parameters determined via fits to the available experimental data using the χ^2 method. The goodness-of-fit is very poor for Scenario S1, which corresponds to the traditional QCDF case without the soft COME contributions, and for Scenario S2, which includes the soft COME contributions but omits the weak annihilation (WA) contributions. Scenario S3, in which both the COME and WA contributions are included simultaneously, achieves an excellent overall fit. In Scenario S3, the QCDF approach can accommodate almost all $B \to \pi\pi$ observables in a consistent and satisfactory manner, and the fitted parameters $\rho_A < 1$ (WA) and $\rho_c \sim 0.3$ (soft COME) are in good agreement with the QCDF power counting scheme and the factorization hypothesis.

DOI: 10.1103/wrm3-6qwv

I. INTRODUCTION

From the perspective of the underlying weak interaction dynamics, the $B \to \pi\pi$ decays are effectively induced by the quark transition $b \to u\bar{u}d$ within the Standard Model (SM) of elementary particle physics. These decays serve as significant and fascinating probes for investigating the origin of CP violation in weak decays of flavored hadrons, and for constraining the angle α sandwiched between the sides $V_{ud}V_{ub}^*$ and $V_{td}V_{tb}^*$ of the most commonly studied unitarity triangle [1–4], where V_{ij} denotes the Cabibbo-Kobayashi-Maskawa (CKM) matrix elements [5,6]. Moreover, the two-body kinematics of the $B \to \pi\pi$ decays are remarkably simple, which facilitates a detailed investigation of weak decay dynamics and the behavior of QCD across different energy regimes, while also providing a foundation for studies of multibody B meson decays.

Over the past years, the $B \to \pi\pi$ decays have attracted considerable interest from both experimental and theoretical communities, leading to numerous significant advances. On the experimental side, a wealth of data on B meson decays is now available and continues to accumulate with steadily improving precision. The most recent experimental results for the branching ratios and CP asymmetries of the $B \to \pi\pi$ decays are summarized in Table I. On the theoretical side, several QCD-improved factorization approaches have been developed to compute hadronic matrix elements (HMEs) effectively, including the QCD factorization (QCDF) approach [7–12] and the perturbative QCD (PQCD) approach [13–20]. Selected branching ratios predicted by these phenomenological approaches are listed in Table II.

A comparison of Tables I and II reveals certain discrepancies between theoretical expectations and experimental measurements of branching ratios. These discrepancies highlight a long-standing unresolved puzzle in nonleptonic B meson decays; how to account simultaneously and consistently for all the $B \to \pi\pi$ observables within the SM, a problem commonly referred to as the "$\pi\pi$ puzzle".

A closer examination of the "$\pi\pi$ puzzle" reveals that the most conspicuous discrepancy lies, in most cases, in the branching ratio for the color-suppressed $B \to \pi^0\pi^0$ decay. As shown in Table II, the inclusion of higher order QCD radiative corrections, extending in some cases to the NNLO level [32], still proves insufficient to reconcile with the experimental data. The theoretical predictions obtained with the QCDF [30–33], SCET [36], and PQCD [37–40] approaches lie significantly below the measured branching ratios. This observation suggests that the discrepancy may originate, at least in part, from overlooked physical mechanisms beyond the perturbative framework. Scenario S1 of the data-driven fit in Ref. [35] is conceptually appealing; however, it requires a relatively large

*Contact author: sunjunfeng@htu.edu.cn

Published by the American Physical Society under the terms of the Creative Commons Attribution 4.0 International license. Further distribution of this work must maintain attribution to the author(s) and the published article's title, journal citation, and DOI. Funded by SCOAP³.

TABLE I. Experimental data on branching ratios and CP asymmetries for the $B \to \pi\pi$ decays.

	PDG [1]	Belle	*BABAR*	Belle II
$10^6 \times \mathcal{B}(\pi^-\pi^0)$	5.31 ± 0.26	5.86 ± 0.46 [21]	5.02 ± 0.54 [22]	5.10 ± 0.40 [23]
$10^6 \times \mathcal{B}(\pi^0\pi^0)$	1.46 ± 0.19	1.31 ± 0.27 [24]	1.83 ± 0.25 [25]	1.25 ± 0.23 [26]
$10^6 \times \mathcal{B}(\pi^+\pi^-)$	5.43 ± 0.26	5.04 ± 0.28 [21]	5.5 ± 0.5 [27]	5.83 ± 0.28 [23]
$\mathcal{A}_{CP}(\pi^-\pi^0)$	-0.01 ± 0.04	0.025 ± 0.044 [21]	0.03 ± 0.08 [22]	-0.081 ± 0.055 [23]
$\mathcal{C}_{CP}(\pi^0\pi^0)$	-0.23 ± 0.18	-0.14 ± 0.37 [24]	-0.43 ± 0.26 [25]	0.05 ± 0.29 [28]
$\mathcal{S}_{CP}(\pi^0\pi^0)$				0.61 ± 0.80 [28]
$\mathcal{C}_{CP}(\pi^+\pi^-)$	-0.314 ± 0.030	-0.33 ± 0.07 [29]	-0.25 ± 0.08 [25]	
$\mathcal{S}_{CP}(\pi^+\pi^-)$	-0.670 ± 0.030	-0.64 ± 0.09 [29]	-0.68 ± 0.10 [25]	

annihilation parameter $\rho_A \sim 3$, which appears implausible within the QCDF approach. Alternatively, by introducing nonperturbative contributions from soft form factors and soft color-octet matrix elements (COME), the improved PQCD calculations in Refs. [41,42] achieve a more favorable comparison with the data. Nevertheless, an inverted hierarchical branching ratio relation, $\mathcal{B}(\pi^+\pi^-) < \mathcal{B}(\pi^-\pi^0)$, is predicted, which is inconsistent with the measurements reported by *BABAR*, Belle II, and the PDG groups, as well as with the majority of theoretical expectations (see Tables I and II). The method/ansatz introduced in Ref. [41] has also been straightforwardly

TABLE II. Theoretical results for branching ratios of the $B \to \pi\pi$ decays. For further details, see the references cited.

Cases		$10^6 \times \mathcal{B}(\pi^-\pi^0)$	$10^6 \times \mathcal{B}(\pi^0\pi^0)$	$10^6 \times \mathcal{B}(\pi^+\pi^-)$
QCDF	Ref. [30]	5.36	0.13	9.97
	Ref. [31][a]	$6.0^{+3.0+2.1+1.0+0.4}_{-2.4-1.8-0.5-0.4}$	$0.3^{+0.2+0.2+0.3+0.2}_{-0.2-0.1-0.1-0.1}$	$8.9^{+4.0+3.6+0.6+1.2}_{-3.4-3.0-1.0-0.8}$
		(5.8, 5.5, 6.0, 5.1)	(0.7, 0.9, 0.4, 0.7)	(6.0, 4.6, 9.5, 5.2)
	Ref. [32][b]	$5.43^{+0.06+1.45}_{-0.06-0.84}$	$0.33^{+0.11+0.42}_{-0.08-0.17}$	$7.37^{+0.86+1.22}_{-0.69-0.97}$
		$(5.82^{+0.07+1.42}_{-0.06-1.35})$	$(0.63^{+0.12+0.64}_{-0.10-0.42})$	$(5.70^{+0.70+1.16}_{-0.55-0.97})$
	Ref. [33][c]	$5.26^{+1.13}_{-1.04}$	$0.39^{+0.09}_{-0.09}$	$5.93^{+1.67}_{-1.47}$
		$(5.89^{+1.25}_{-1.23})$	$(0.98^{+0.44}_{-0.31})$	$(5.60^{+1.19}_{-1.68})$
	Ref. [34]	$5.9^{+2.2+1.4}_{-1.1-1.1}$	$1.1^{+1.0+0.7}_{-0.4-0.3}$	$7.0^{+0.4+0.7}_{-0.7-0.7}$
	Ref. [35][d]	$(5.20^{+0.64+1.11}_{-0.47-1.00})$	$(1.67^{+0.22+0.25}_{-0.19-0.23})$	$(5.88^{+0.66+1.66}_{-0.49-1.45})$
		$[5.59^{+0.68+1.15}_{-0.51-1.04}]$	$[2.13^{+0.29+0.32}_{-0.24-0.29}]$	$[5.74^{+0.64+1.63}_{-0.47-1.42}]$
SCET	Ref. [36]	$5.2 \pm 1.6 \pm 2.1 \pm 0.6$	$0.84 \pm 0.29 \pm 0.30 \pm 0.19$	$5.4 \pm 1.3 \pm 1.4 \pm 0.4$
PQCD	Ref. [37]	$4.27^{+1.85}_{-1.47}$	$0.23^{+0.19}_{-0.15}$	$7.67^{+3.47}_{-2.64}$
	Ref. [38][e]	$3.35^{+1.08+0.23}_{-0.77-0.22}$	$0.29^{+0.11+0.03}_{-0.07-0.02}$	$6.19^{+2.09+0.38}_{-1.48-0.34}$
		$(4.45^{+1.38+0.39}_{-0.99-0.36})$	$(0.61^{+0.16+0.14}_{-0.12-0.12})$	$(5.39^{+1.86+0.28}_{-1.31-0.25})$
	Ref. [39][f]	$(3.04^{+0.18+0.16+0.27}_{-0.17-0.16-0.25})$	$(0.24^{+0.02+0.04+0.01}_{-0.02-0.03-0.01})$	$(5.52^{+0.34+0.37+0.47}_{-0.32-0.36-0.43})$
		$[3.23^{+0.19+0.18+0.29}_{-0.18-0.18-0.27}]$	$[0.24^{+0.02+0.04+0.01}_{-0.02-0.04-0.01}]$	$[5.82^{+0.36+0.41+0.50}_{-0.34-0.39-0.46}]$
		$\{3.42^{+0.21+0.20+0.32}_{-0.19-0.20-0.30}\}$	$\{0.23^{+0.02+0.04+0.01}_{-0.02-0.04-0.01}\}$	$\{6.12^{+0.39+0.45+0.54}_{-0.36-0.43-0.50}\}$
	Ref. [40]	$4.18^{+1.32}_{-0.97}$	$0.23^{+0.07}_{-0.05}$	$7.31^{+2.38}_{-1.72}$
	Ref. [41]	$5.72 \pm 0.44^{+0.29}_{-0.37}$	$1.50 \pm 0.24^{+0.18}_{-0.19}$	$5.14 \pm 0.61^{+0.34}_{-0.37}$
	Ref. [42]	$5.63 \pm 0.53^{+0.12+0.19}_{-0.23-0.20}$	$1.41 \pm 0.35^{+0.04+0.12}_{-0.06-0.17}$	$5.14 \pm 0.69^{+0.16+0.28}_{-0.25-0.24}$

[a]Numbers in parentheses correspond to four different scenarios.
[b]The NNLO vertex corrections are considered. Numbers in parentheses correspond to the favored results.
[c]Numbers in parentheses are obtained by applying the principle of maximum conformality.
[d]Numbers in round and square brackets correspond to the S1 and S2 scenarios, respectively.
[e]Numbers in parentheses include the Glauber-gluon effect.
[f]Numbers in round, square and curly brackets correspond to the S1, S2, and S3 scenarios, respectively.

TABLE III. Input parameters, where the central values are regarded as the default inputs unless specified otherwise.

Particle mass	Decay constant	Wolfenstein parameters
$m_{\pi^\pm} = 139.57$ MeV [1],	$f_\pi = 130.2 \pm 1.2$ MeV [1],	$A = 0.826^{+0.017}_{-0.015}$ [1],
$m_{\pi^0} = 134.977$ MeV [1],	$f_B = 189.5 \pm 1.3$ MeV [1];	$\lambda = 0.22517 \pm 0.00068$ [1],
$m_b = 4.788 \pm 0.016$ GeV [1],	Life time	$\bar{\rho} = 0.1576^{+0.0092}_{-0.0091}$ [1],
$m_{B^\pm} = 5279.41 \pm 0.07$ MeV [1],	$\tau_{B^\pm} = 1.638 \pm 0.004$ ps [1],	$\bar{\eta} = 0.3556^{+0.0071}_{-0.0069}$ [1];
$m_{B^0} = 5279.63 \pm 0.20$ MeV [1];	$\tau_{B^0} = 1.5116 \pm 0.0031$ ps [1];	
Parameters of wave function	$\lambda_B = 350 \pm 150$ MeV [12],	$a_2^\pi = 0.25 \pm 0.15$ [98].

generalized to other nonleptonic two-body B meson decays within the modified PQCD approach, achieving improved agreement between theoretical calculations and experimental measurements [42–47]. It is conceivable that some of the insights gleaned from these investigations could be profitably employed to refine the QCDF calculations.

It is worth noting that COME contributions are closely related to the rationale for the conventional factorization approximation and to the dynamical understanding of color selection rules in exclusive nonleptonic meson weak decays. These contributions have been extensively discussed and investigated in connection with apparent discrepancies between theoretical predictions and experimental results in numerous works, including Refs. [41–94]. In this paper, we will revisit and reassess the soft COME contributions as a means of reinvestigating the $B \to \pi\pi$ decays within the QCDF framework. Our objectives are twofold; first, to ascertain whether this ingredient can alleviate the tensions inherent in the "$\pi\pi$ puzzle", and second, to explore the extent to which soft COME contributions are empirically supported by the available data.

The remainder of this paper is organized as follows. Section II delineates the theoretical framework for the $B \to \pi\pi$ decays. The numerical results and discussion are presented in Sec. III. A brief summary is given in Sec. IV.

II. THEORETICAL FRAMEWORK FOR THE $B \to \pi\pi$ DECAYS

A. The effective Hamiltonian

By means of the operator product expansion and the renormalization group (RG) techniques, the effective Hamiltonian governing the nonleptonic $B \to \pi\pi$ decays can be expressed as a sum of local four-quark operators O_i, each multiplied by the corresponding Wilson coefficients C_i and products of the CKM matrix elements V_{ij}. More specifically, this effective Hamiltonian takes the form [95],

$$\mathcal{H}_{\rm eff} = \frac{G_F}{\sqrt{2}} \sum_{p=u,c} V_{pb} V_{pd}^* \left\{ \sum_{i=1}^{2} C_i(\mu) O_i^p + \sum_{j=3}^{10} C_j(\mu) O_j \right\} + \text{H.c.}, \tag{1}$$

where $G_F \approx 1.166 \times 10^{-5}$ GeV^{-2} [1] is the Fermi coupling constant. Employing the Wolfenstein parametrization [96,97], the relevant CKM factors are expressed, up to order $\mathcal{O}(\lambda^7)$, as follows:

$$V_{ub} V_{ud}^* = A\lambda^3(\bar{\rho} - i\bar{\eta}) + \mathcal{O}(\lambda^7), \tag{2}$$

$$V_{cb} V_{cd}^* = -A\lambda^3 + \mathcal{O}(\lambda^7), \tag{3}$$

$$V_{tb} V_{td}^* = A\lambda^3(1 - \bar{\rho} + i\bar{\eta}) + \mathcal{O}(\lambda^7). \tag{4}$$

The global fit results for the Wolfenstein parameters A, λ, $\bar{\rho}$, and $\bar{\eta}$ are displayed in Table III. The Wilson coefficients C_i encode the short-distance physics contributions arising from gluon exchanges with virtualities above the scale μ, and are calculated using RG-improved perturbation theory, owing to the asymptotic freedom of QCD. Their numerical values, including both the leading-order (LO) and next-to-leading-order (NLO) corrections within the naïve dimensional regularization (NDR) scheme, are shown in Table IV. The relevant operators governing the decays under consideration are expressed as follows:

$$O_1^p = (\bar{p}_\alpha b_\alpha)_{V-A} (\bar{d}_\beta p_\beta)_{V-A}, \tag{5}$$

$$O_2^p = (\bar{p}_\alpha b_\beta)_{V-A} (\bar{d}_\beta p_\alpha)_{V-A}, \tag{6}$$

$$O_{i=3,9} = (\bar{d}_\alpha b_\alpha)_{V-A} \sum_q \left(\delta_{i,3} + \delta_{i,9} \frac{3}{2} Q_q \right) (\bar{q}_\beta q_\beta)_{V-A}, \tag{7}$$

$$O_{i=4,10} = (\bar{d}_\alpha b_\beta)_{V-A} \sum_q \left(\delta_{i,4} + \delta_{i,10} \frac{3}{2} Q_q \right) (\bar{q}_\beta q_\alpha)_{V-A}, \tag{8}$$

$$O_{i=5,7} = (\bar{d}_\alpha b_\alpha)_{V-A} \sum_q \left(\delta_{i,5} + \delta_{i,7} \frac{3}{2} Q_q \right) (\bar{q}_\beta q_\beta)_{V+A}, \tag{9}$$

$$O_{i=6,8} = (\bar{d}_\alpha b_\beta)_{V-A} \sum_q \left(\delta_{i,6} + \delta_{i,8} \frac{3}{2} Q_q \right) (\bar{q}_\beta q_\alpha)_{V+A}, \tag{10}$$

where we use the shorthand notation $(\bar{q}_1 q_2)_{V\pm A} \equiv \bar{q}_1 \gamma_\mu (1 \pm \gamma_5) q_2$, α and β are the color indices, Q_q is the

TABLE IV. Numerical values of the Wilson coefficients C_i in the NDR scheme, with input parameters taken as the W boson mass $m_W = 80.3625 \pm 0.0077$ GeV [1], the top quark mass $m_t = 172.60 \pm 0.27$ GeV [1], the typical scale $\Lambda_h = 0.5$ GeV [12], $\alpha_{\rm em}^{-1}(\mu_h) \approx 128.8$, and $\alpha_{\rm em}^{-1}(\mu_b) \approx 128.6$. Unless explicitly stated otherwise, the central values of these inputs are adopted as the default.

	$\mu_h = \sqrt{m_b \Lambda_h}$		$\mu_b = m_b$	
	LO	NLO	LO	NLO
C_1	1.220	1.174	1.110	1.076
C_2	−0.421	−0.348	−0.237	−0.173
C_3	0.025	0.027	0.012	0.014
C_4	−0.058	−0.059	−0.032	−0.034
C_5	0.011	0.011	0.008	0.008
C_6	−0.077	−0.080	−0.037	−0.039
$C_7/\alpha_{\rm em}$	−0.103	−0.018	−0.096	0.004
$C_8/\alpha_{\rm em}$	0.032	0.108	0.014	0.052
$C_9/\alpha_{\rm em}$	−0.091	−1.432	−0.090	−1.297
$C_{10}/\alpha_{\rm em}$	−0.030	0.455	−0.018	0.249

electric charge of quark q in the unit of $|e|$, and $q \in \{u, d, c, s, b\}$.

B. The $B \to \pi\pi$ decays with the naive factorization approach

The understanding of nonleptonic decays is handicapped by the influence of the strong interactions. The HME, in which the local operators O_i are sandwiched between the initial B meson and the final $\pi\pi$ pair, characterizes the transition from quarks to hadrons. It receives both perturbative and nonperturbative contributions, and thus constitutes the most challenging part of the theoretical calculation.

An oversimplified phenomenological description is provided by the naïve factorization (NF) hypothesis [99–105], whose physical foundation rests on the "color transparency" argument for energetic nonleptonic decays [106], together with the vacuum-insertion approximation and the valence quark decay assumption. Within the NF framework, the HMEs of four-quark operators are factorized into products of two HMEs of flavor-matched color-singlet diquark currents. These factorized products are subsequently parametrized in terms of two fundamental hadronic observables; the decay constant and the form factor. More specifically, for the $B \to \pi^+\pi^-$ decay, we decompose the HME of the operator O_1^u as follows:

$$\langle O_1^u \rangle = \langle \pi^+\pi^- | O_1 | B \rangle = \langle O_1^u \rangle_{\rm f} + \langle O_1^u \rangle_{\rm nf}, \tag{11}$$

where the subscripts "f" and "nf" denote the factorizable and nonfactorizable contributions, respectively. With the NF approach, the factorizable part reads [105,107],

$$\langle O_1^u \rangle_{\rm f} = \langle \pi^- | (\bar{d}_\beta u_\beta)_{V-A} | 0 \rangle \langle \pi^+ | (\bar{u}_\alpha b_\alpha)_{V-A} | B \rangle, \tag{12}$$

$$\langle \pi^- | (\bar{d}_\beta u_\beta)_{V-A} | 0 \rangle = -i f_\pi p_{\pi^-}^\mu, \tag{13}$$

$$\langle \pi^+ | (\bar{u}_\alpha b_\alpha)_{V-A} | B \rangle = \left(p_B^\mu + p_{\pi^+}^\mu - \frac{m_B^2 - m_\pi^2}{q^2} q^\mu \right) F_1^{B\pi}(q^2) + \frac{m_B^2 - m_\pi^2}{q^2} q^\mu F_0^{B\pi}(q^2), \tag{14}$$

where f_π is the pion decay constant, $q^\mu = p_B^\mu - p_{\pi^+}^\mu$ is the momentum transfer, the $B \to \pi$ transition form factors $F_{0,1}^{B\pi}$ are scalar functions of q^2, and satisfy the condition $F_0^{B\pi}(0) = F_1^{B\pi}(0)$ at $q^2 = 0$, thereby ensuring the absence of pole singularity.

In the $1/N_c$ expansion, where N_c denotes the number of colors, the factorizable amplitude is of order $\mathcal{O}(\sqrt{N_c})$, while the nonfactorizable one is of order $\mathcal{O}(1/\sqrt{N_c})$ [58]. Using the RG equation for the Wilson coefficients, one finds that the ratio [80] is

$$\varepsilon_1 = \frac{\langle O_1^u \rangle_{\rm nf}}{\langle O_1^u \rangle_{\rm f}} = \mathcal{O}\left(\frac{1}{N_c^2} \right). \tag{15}$$

By employing the identity relationship among the generators T^a (with $a = 1, \ldots, 8$) of the $SU(3)$ color group,

$$T_{i,j}^a T_{k,l}^a = \frac{1}{2} \delta_{i,l} \delta_{k,j} - \frac{1}{2N_c} \delta_{i,j} \delta_{k,l}, \tag{16}$$

where the subscripts i, j, k, l are color indices, the operator O_2^u can be equivalently recast as follows:

$$\begin{aligned} O_2^u &= (\bar{u}_\alpha b_\beta)_{V-A} (\bar{d}_\beta u_\alpha)_{V-A} \\ &= \frac{1}{N_c} (\bar{u}_\alpha b_\alpha)_{V-A} (\bar{d}_\beta u_\beta)_{V-A} + 2 (\bar{u} T^a b)_{V-A} (\bar{d} T^a u)_{V-A} \\ &= \frac{1}{N_c} O_1^u + 2 \tilde{O}_2^u, \end{aligned} \tag{17}$$

The operator $\tilde{O}_2^u$ is composed of two color-octet currents,

$$\tilde{O}_2^u = (\bar{u} T^a b)_{V-A} (\bar{d} T^a u)_{V-A}. \tag{18}$$

The evaluations in Ref. [80] show that the ratio is

$$\varepsilon_8 = 2 \frac{\langle \tilde{O}_2^u \rangle}{\langle O_1^u \rangle_{\rm f}} = \mathcal{O}\left(\frac{1}{N_c} \right). \tag{19}$$

The contribution of $\langle \tilde{O}_2^u \rangle$, whose color configuration does not match that of the participating hadrons under the vacuum-insertion approximation, is completely discarded by the NF approach.

There exists, in principle, another type of factorizable contribution, the so-called "weak annihilation (WA)

contribution". For example, by applying the Fierz rearrangement to the products of two color-mismatched diquark currents, one obtains the following factorized form:

$$\begin{aligned}\langle O_2^u\rangle_a &= \langle\pi^+\pi^-|(\bar{u}_\alpha b_\beta)_{V-A}(\bar{d}_\beta u_\alpha)_{V-A}|B\rangle_a \\ &= \langle\pi^+\pi^-|(\bar{u}_\alpha u_\alpha)_{V-A}(\bar{d}_\beta b_\beta)_{V-A}|B\rangle_a \\ &= \langle\pi^+\pi^-|(\bar{u}_\alpha u_\alpha)_{V-A}|0\rangle\langle 0|(\bar{d}_\beta b_\beta)_{V-A}|B\rangle, \end{aligned} \tag{20}$$

where the subscript "a" denotes the WA contribution. The WA contributions are formally disregarded in the NF approach on the basis of helicity suppression arguments [108] or the $1/m_b$ power counting rules in the heavy quark limit [8]. In addition, as stated in Ref. [80], the "color transparency" argument precludes the possibility of significant final state interactions for the energetic $B \to \pi\pi$ decays.

To summarize, within the NF scheme, no attempt is made to include nonfactorizable contributions, terms beyond the $1/N_c$ expansion, and WA amplitudes. Adopting the conventions for the HMEs defined in Eqs. (12)–(14), the decay amplitudes for the $B \to \pi\pi$ processes can be expressed as follows:

$$\mathcal{F}_{\pi\pi} = \frac{G_F}{\sqrt{2}}\langle\pi^+\pi^-|O_1^u|B\rangle_f = -i\frac{G_F}{\sqrt{2}}(m_B^2 - m_\pi^2) f_\pi F_0^{B\pi}(m_\pi^2), \tag{21}$$

$$\mathcal{M}_{+-}^f = \mathcal{F}_{\pi\pi}\{V_{ub}V_{ud}^* a_1 - V_{tb}V_{td}^*(a_4 + a_{10} + a_6 r_\pi + a_8 r_\pi)\}, \tag{22}$$

$$\begin{aligned}\mathcal{M}_{-0}^f = \frac{\mathcal{F}_{\pi\pi}}{\sqrt{2}}\Big\{ & V_{ub}V_{ud}^*(a_1 + a_2) \\ & - V_{tb}V_{td}^*\frac{3}{2}(a_9 + a_{10} - a_7 + a_8 r_\pi)\Big\}, \end{aligned} \tag{23}$$

$$\begin{aligned}\mathcal{M}_{00}^f = -\mathcal{F}_{\pi\pi}\Big\{ & V_{ub}V_{ud}^* a_2 + V_{tb}V_{td}^*\Big(a_4 + a_6 r_\pi + \frac{3}{2}a_7 \\ & - \frac{1}{2}a_8 r_\pi - \frac{3}{2}a_9 - \frac{1}{2}a_{10}\Big)\Big\}, \end{aligned} \tag{24}$$

where the superscript "f" attached to $\mathcal{M}_{ij}^f$ designates the factorizable amplitude, and the subscripts "i" and "j" specify the isospin z-component of the pions. The coefficient is given by the following combination of Wilson coefficients:

$$a_i = C_i + \frac{1}{N_c}C_j, \tag{25}$$

with $j = i - 1$ for even i, and $j = i + 1$ for odd i. The chiral factor $r_\pi = m_\pi^2/[\bar{m}_b(\mu)\bar{m}_q(\mu)]$ is computed via the RG equation for the "running mass", with inputs $\bar{m}_b(\bar{m}_b) = 4.1859 \pm 0.0034$ GeV and $\bar{m}_q(2\text{ GeV}) = \frac{1}{2}(\bar{m}_u + \bar{m}_d) = 3.49 \pm 0.04$ MeV [1].

The NF scheme suffers from several inherent drawbacks. The first concerns the renormalization scale dependence. The HME in Eq. (21) is independent of the renormalization scale μ, which implies that the μ dependence of the Wilson coefficients remains uncompensated. Consequently, the resulting decay amplitudes are scale ambiguous and hence unphysical. The second issue is the complete neglect of nonfactorizable contributions. This omission is likely responsible for the inadequacy of the NF approach, particularly in describing color-suppressed B decays and CP asymmetries; consequently, the coefficient a_2 becomes highly sensitive to any additional nonfactorizable effects. The third deficiency is that the decay amplitudes are entirely devoid of strong phases, even though such phases are crucial for reproducing the observed CP asymmetries in exclusive nonleptonic B decays.

C. The $B \to \pi\pi$ decays with the QCDF approach

The aforementioned shortcomings of the NF scheme are largely addressed by the QCDF approach [8–12]. Following the factorization approach for exclusive hadronic processes proposed in Ref. [109] and the master QCDF formula [8], HMEs can be approximated, up to the power corrections of order $1/m_b$, as convolutions of scattering kernels with wave functions of the participating mesons,

$$\begin{aligned}\langle\pi_1\pi_2|O_i|B\rangle = {} & F_0^{B\pi}(m_\pi^2) f_\pi\Big\{\int dy\, \mathcal{T}^I(y)\Phi_{\pi_1}(y) \\ & + \int dz\, \mathcal{T}^I(z)\Phi_{\pi_2}(z)\Big\} \\ & + f_B f_\pi^2 \int dx\, dy\, dz\, \mathcal{T}^{II}(x,y,z)\Phi_B(x) \\ & \times \Phi_{\pi_1}(y)\Phi_{\pi_2}(z), \end{aligned} \tag{26}$$

where the nonperturbative quantities $F_0^{B\pi}$ and f_π are the form factor and pion decay constant specified in Eqs. (14) and (13), respectively. The functions $\mathcal{T}^I$ and $\mathcal{T}^{II}$ are the scattering kernels that account for the hard gluon exchange interactions among the quarks and are reliably calculable in perturbative QCD. Φ_i is the universal meson wave function. The variables x, y, and z denote the longitudinal momentum fractions of valence quarks.

The calculation yields the effective QCDF coefficients a_i^p [12],

$$a_i^p = a_{i,I}^p + a_{i,II}, \tag{27}$$

where $a_{i,I}^p$ (with $p = u, c$) correspond to the form factor terms in Eq. (26) and contain the NF contributions as well as the vertex and penguin corrections, while $a_{i,II}$ arises

TABLE V. Numerical values of the NLO coefficients $a_{i,I}^p$ at the scale $\mu = m_b$.

$a_{1,I}^p = 1.052 + i0.017$	$a_{2,I}^p = 0.027 - i0.080$	$a_{3,I}^p = 0.007 + i0.002$
$-a_{4,I}^u = 0.036 + i0.015$	$-a_{4,I}^c = 0.039 + i0.004$	$-a_{5,I}^p = 0.006 + i0.003$
$-a_{6,I}^u = 0.042 + i0.014$	$-a_{6,I}^c = 0.045 + i0.003$	$a_{7,I}^p/\alpha_{\rm em} = 0.022 + i0.001$
$a_{8,I}^u/\alpha_{\rm em} = 0.053 - i0.010$	$a_{8,I}^c/\alpha_{\rm em} = 0.051 - i0.004$	$-a_{9,I}^p/\alpha_{\rm em} = 1.212 - i0.001$
$-a_{10,I}^u/\alpha_{\rm em} = 0.176 + i0.003$	$-a_{10,I}^c/\alpha_{\rm em} = 0.178 - i0.003$	

from the hard spectator scattering (HSS) interactions. The explicit analytic expressions for the QCDF coefficients a_i^p at NLO are available in Ref. [12], and their numerical values for $a_{i,I}^p$ are listed in Table V. It is evident that the QCDF coefficients $a_{i,I}^p$ (or a_i^p) at NLO contain nonzero imaginary parts. The partial strong rescattering phases are successfully reproduced by taking into account the nonfactorizable contributions within the QCDF approach. It has been shown in Refs. [8–11] that the QCDF coefficients $a_{i,I}^p$ are gauge invariant, infrared finite, and independent of the renormalization scale at order α_s. The residual scale dependence observed in the numerical results of Table 3 in Ref. [12] is entirely attributable to the truncation of the perturbative series. In this work, we adopt the NLO coefficients given in Ref. [12] for the subsequent calculations. The detailed expressions and values for the QCDF coefficients a_i^p at NNLO for the $B \to \pi\pi$ decays can be found in Refs. [32,110].

As demonstrated in Refs. [30–32,34–42], the WA contributions are numerically significant and indispensable for both the branching ratios and the CP asymmetries in the $B \to \pi\pi$ decays, irrespective of whether the QCDF or PQCD approach is employed. In this work, we adopt the prescription of Ref. [12] for the WA HMEs in terms of convolutions of scattering kernels with light-cone distribution amplitudes (LCDAs) of the participating mesons, and take the WA contributions into account accordingly. The explicit expressions for the WA amplitudes $\mathcal{M}_{\pi\pi}^a$ can be found in Refs. [30,31] and are not reproduced here for brevity. For consistency throughout this work, we have revised the parametric expressions for the basic WA building blocks originally presented in Ref. [12] by including the truncation at $n = 2$ in the Gegenbauer polynomial expansion of the pion twist-2 LCDAs, in analogy with the treatment of the vertex corrections and HSS contributions to the QCDF coefficients a_i^p. The modified expressions for the WA building blocks are as follows:

$$\begin{aligned} A_{1,2}^i = \pi\alpha_s\{&2r_\pi^2 X_A^2 + 6[3X_A + \pi^2 - 12 \\ &+ (21X_A + 42\pi^2 - 464)a_2^\pi \\ &+ (18X_A + 2916\pi^2 - 28827)(a_2^\pi)^2]\}, \end{aligned} \tag{28}$$

$$A_3^f = 12\pi\alpha_s r_\pi X_A\{2X_A - 1 + (12X_A - 31)a_2^\pi\}, \tag{29}$$

where the quantities $A_k^{i,f}$ have the same meanings as those in Eq. (62) of Ref. [12]. The Gegenbauer moment a_2^π is closely related to the pion twist-2 LCDAs, which are conventionally expanded in terms of the Gegenbauer polynomials as [98]

$$\Phi_\pi(x) = 6x\bar{x}\sum_{n=0} a_n^\pi C_n^{3/2}(x - \bar{x}), \tag{30}$$

where x and $\bar{x} = 1 - x$ denote the longitudinal momentum fractions carried by the valence quarks inside the pion, with $a_0^\pi = 1$ and $a_1^\pi = 0$ by virtue of isospin symmetry and G-parity. The quantity X_A is defined as follows [12,31]:

$$X_A = \int_0^1 \frac{dx}{x} = (1 + \rho_A e^{i\phi_A}) \ln\frac{m_B}{\Lambda_h}, \tag{31}$$

where the scale is set to $\Lambda_h = 0.5$ GeV, and ϕ_A is an arbitrary phase that may arise from soft rescattering effects. As proposed in Refs. [12,31], the condition $\rho_A < 1$ is generally imposed to guarantee the reliability of the convolution treatment for the WA HMEs within the QCDF framework.

Besides the WA endpoint divergence discussed above, an analogous endpoint divergence also appears in the HSS amplitudes. This divergence is handled using a similar parametrization scheme [12,31],

$$X_H = (1 + \rho_H e^{i\phi_H}) \ln\frac{m_B}{\Lambda_h}, \tag{32}$$

with the same phenomenological interpretation for the parameters ρ_H and ϕ_H as in the WA case. It should be noted, however, that the parameters X_H and X_A are in principle independent. They are associated with convolution integrals over pion LCDAs of different twists and correspond to distinct topological structures, and therefore should not be identified with each other. Moreover, the parameters $X_{A,H}$ can be further split into multiple parameters according to different topological structures (see, e.g., Refs. [35,111–114]) or, alternatively, according to different final states (see, e.g., Refs. [31,34,115]). Such arbitrariness inevitably introduces considerable theoretical uncertainties and significantly undermines the predictive power of the QCDF approach. Since only the $\pi\pi$ final states are considered here, and in view of the constraints from isospin symmetry as well as the limited number of available

experimental data, we will adopt the convention of Ref. [12] to reduce the number of free parameters. Thus, for the time being, we take $X_H = X_A$.

D. The soft COME contributions to the $B \to \pi\pi$ decays

From the detailed analysis of the nonfactorizable contributions to the $B \to D\pi$ process in Ref. [8], it is evident that the hard COME contributions of the operator $\tilde{O}_2^c$ (denoted as O_8 in Ref. [8]) correspond to the vertex corrections encoded in the coefficients $a_{i,I}^c$. For the $B \to \pi\pi$ decays, the hard COME contributions from the $\tilde{O}_2^p$-like operators have been consistently incorporated into the effective QCDF coefficient a_i^p in Eq. (27). However, the soft COME contributions have not yet been thoroughly investigated. Although it was estimated in Ref. [8] that they are power suppressed relative to the hard ones in the HSS amplitudes, their numerical importance cannot be excluded *a priori* for realistic B meson decays, given that m_b is not asymptotically large. It is therefore worthwhile to investigate whether such soft nonperturbative effects could play a role in the $B \to \pi\pi$ decays. Given the nonperturbative nature of soft COME contributions, we do not attempt to evaluate them using nonperturbative methods, such as the QCD sum rules employed in Ref. [62]. Instead, following the strategy proposed in Refs. [41,80], we parametrize the ratio of the soft COME to the factorizable color-singlet HME in terms of a complex parameter X_c, defined as

$$X_c = \frac{\langle \tilde{O}_2^u \rangle_{\rm soft}}{\langle O_1^u \rangle_{\rm f}} = \rho_c e^{i\phi_c}, \tag{33}$$

where ρ_c and ϕ_c are assumed to be universal for the $B \to \pi\pi$ decays, based on isospin symmetry in the strong interactions. Consequently, the decay amplitudes arising solely from soft COME contributions can be expressed as

$$\mathcal{M}_{\pi\pi}^c = 2X_c \mathcal{M}_{\pi\pi}^f(a_i \to C_j^{\rm NLO}(\mu_f)), \tag{34}$$

where $j = i - 1$ for even i, and $j = i + 1$ for odd i; the factorizable decay amplitudes $\mathcal{M}_{\pi\pi}^f$ have been given in Eqs. (22)–(24). The factorization scale μ_f serves to separate perturbative and nonperturbative contributions. In analogy with the treatment of the scale in WA amplitudes within the QCDF framework, we adopt the approximation $\mu_f = \mu_h$ in this work to bridge the hard and soft contributions, and we do not dwell on the μ_f scale dependence for the moment. As can be seen from Eq. (34), the soft COME amplitude for the $B \to \pi^0\pi^0$ ($\pi^+\pi^-$) decay is proportional to the coefficient C_1 (C_2), and thus would significantly (mildly) affect the branching ratio and CP asymmetries. This observation suggests a possible alternative mechanism for accommodating the "$\pi\pi$ puzzle" within the QCDF approach.

Based on the above analysis, the decay amplitudes, including the hard and soft nonfactorizable COME effects as well as the WA contributions, can be written as

$$\mathcal{M}_{\pi\pi} = \mathcal{M}_{\pi\pi}^f + \mathcal{M}_{\pi\pi}^a + \mathcal{M}_{\pi\pi}^c. \tag{35}$$

III. NUMERICAL RESULTS AND DISCUSSION

To quantitatively assess the contributions from the factorizable, nonfactorizable, WA, and soft COME amplitudes, we employ the least-squares method to construct estimators for the unknown parameters by making full use of the PDG data. The chi-square function is defined as

$$\chi_i = \frac{y_{i,\rm theo.} - y_{i,\rm exp.}}{\sigma_i}, \tag{36}$$

$$\chi^2 = \sum_i \chi_i^2, \tag{37}$$

where y_i denotes the branching ratios and CP asymmetries, and σ_i is the corresponding experimental uncertainty. The experimental data $y_{i,\rm exp.}$ and errors σ_i are listed in Table I. The closer the absolute value of χ_i is to zero, the better the agreement between the theoretical predictions and the experimental results.

The branching ratio is computed as

$$\mathcal{B} = \frac{p_{\rm cm}}{16\pi} \frac{\tau_B}{m_B^2} (|\mathcal{M}_{\pi\pi}|^2 + |\overline{\mathcal{M}}_{\pi\pi}|^2), \tag{38}$$

where $p_{\rm cm}$ is the pion momentum in the rest frame of the decaying B meson, τ_B is the B meson lifetime, and $\overline{\mathcal{M}}_{\pi\pi}$ denotes the Hermitian conjugate of the amplitude given in Eq. (35).

For charged B decays, the direct CP asymmetry is given by

$$\mathcal{A}_{CP} = \frac{|\mathcal{M}(B^- \to \pi^-\pi^0)|^2 - |\mathcal{M}(B^+ \to \pi^+\pi^0)|^2}{|\mathcal{M}(B^- \to \pi^-\pi^0)|^2 + |\mathcal{M}(B^+ \to \pi^+\pi^0)|^2}. \tag{39}$$

For neutral B decays, the time-dependent CP asymmetry is given by

$$\begin{aligned} \mathcal{A}_{CP} &= \frac{|\mathcal{M}(\bar{B}^0 \to \pi\pi)|^2 - |\mathcal{M}(B^0 \to \pi\pi)|^2}{|\mathcal{M}(\bar{B}^0 \to \pi\pi)|^2 + |\mathcal{M}(B^0 \to \pi\pi)|^2} \\ &= \mathcal{S}_{CP} \sin(\Delta m_d t) - \mathcal{C}_{CP} \cos(\Delta m_d t), \end{aligned} \tag{40}$$

where Δm_d is the mass difference between the two physical B_d meson eigenstates, corresponding to the $B^0 - \bar{B}^0$ oscillation frequency. The mixing-induced and direct CP asymmetry parameters, $\mathcal{S}_{CP}$ and $\mathcal{C}_{CP}$, are respectively defined as

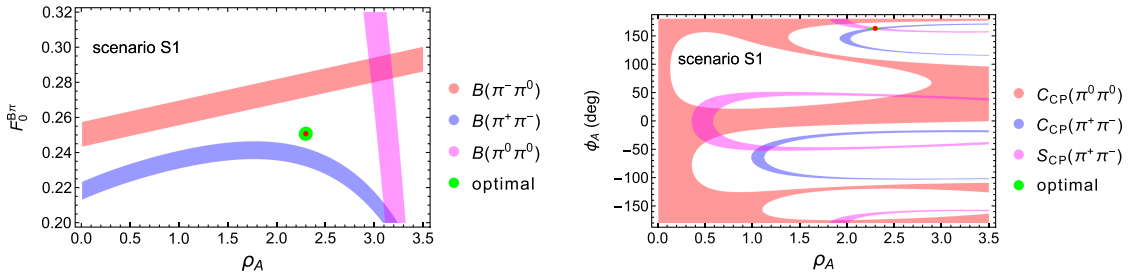


FIG. 1. Constraints on the S1 parameters. The bands represent the parameter regions allowed by the PDG data within the quoted uncertainties, the green oval corresponds to the 1σ range of the fitted parameters, and the red dot indicates the central value of the best-fit solution.

$$\lambda_{CP} = \frac{V_{td}V_{tb}^*}{V_{td}^*V_{tb}} \frac{\mathcal{M}(\bar{B}^0 \to \pi\pi)}{\mathcal{M}(B^0 \to \pi\pi)}, \tag{41}$$

$$\mathcal{S}_{CP} = \frac{2\,\mathrm{Im}(\lambda_{CP})}{1+|\lambda_{CP}|^2}, \tag{42}$$

$$\mathcal{C}_{CP} = \frac{1-|\lambda_{CP}|^2}{1+|\lambda_{CP}|^2}. \tag{43}$$

The free nonperturbative parameters in our fit include the form factor $F_0^{B\pi}$, the WA parameter $X_A = X_H$ (parametrized by ρ_A and ϕ_A), and the soft COME parameter X_c (parametrized by ρ_c and ϕ_c). All other parameters are fixed to their central values as listed in Table III. This choice is based on the following considerations: (1) On the one hand, the available experimental measurements are limited, both in terms of the number of observables and their precision. For example, the relative uncertainties given by the PDG group are 13% for the branching ratio $\mathcal{B}(\pi^0\pi^0)$, and 78% and 400% for the CP asymmetries $\mathcal{C}_{CP}(\pi^0\pi^0)$ and $\mathcal{A}_{CP}(\pi^-\pi^0)$, respectively (see Table I). Given these circumstances, it is challenging to impose tight constraints on the theoretical model parameters, and an excessive number of free parameters would inevitably introduce additional uncertainties into the fit; (2) On the other hand, except for the Gegenbauer moment a_2^π and the inverse moment of the B meson LCDA λ_B, all other input parameters in Table III have already been determined with high precision, and the existing $B \to \pi\pi$ decay measurements alone are insufficient to further improve their constraints. To explore the impact of different assumptions, we consider the following three scenarios:

(1) Scenario S1 ("universal WA"): In this scenario, we set the soft COME amplitude $\mathcal{M}_{\pi\pi}^c = 0$ in Eq. (35) and $X_H = X_A$, which corresponds to the conventional QCDF prescription. The free parameters are $F_0^{B\pi}$, ρ_A, and ϕ_A;
(2) Scenario S2 ("universal soft COME"): In this scenario, we set the WA amplitude $\mathcal{M}_{\pi\pi}^a = 0$ in Eq. (35) and the QCDF coefficient $a_{i,II} = 0$ in Eq. (27), thus excluding the HSS contributions. The free parameters are $F_0^{B\pi}$, ρ_c, and ϕ_c;
(3) Scenario S3 ("combined"): In this scenario, we take into account both the WA and soft COME amplitudes, as well as the interference between them. The free parameters are $F_0^{B\pi}$, ρ_A, ϕ_A, ρ_c, and ϕ_c. This is our favored scenario.

Scenarios S1 and S2 serve as control cases for comparison with our favored Scenario S3. The goodness-of-fit for these two scenarios is substantially worse than that for Scenario S3. Given such poor fits, the best-fit parameter values obtained in Scenarios S1 and S2 are essentially meaningless, and no serious physical conclusions can be drawn from Scenarios S1 and S2, other than that they fail to account for the experimental data. Accordingly, for these two scenarios we report only the corresponding qualitative conclusions, and we refrain from extensive analysis and discussion of their fitted results, since a detailed discussion of poorly fitted scenarios would be of limited value.

A. Scenario S1

The constraints on the form factor $F_0^{B\pi}$ and the parameter ρ_A are mainly derived from the measurements of branching ratios. Since CP asymmetries are defined as ratios of the squared amplitudes, they exhibit a very weak dependence on the form factors. Figure 1 displays the respective constraints imposed by these two types of observables on the parameter space. It is clearly seen that the resulting fits cannot yield a consistent and physically satisfactory interpretation of the measured branching ratios.

The optimal values of the free parameters obtained with the PDG data for Scenario S1, together with their corresponding correlation coefficients, are shown in Table VI. The best-fit values of the WA parameters ρ_A and ϕ_A are illustrated in Fig. 2. Scenario S1 exhibits two distinctive features. The first is that the WA contributions can provide a sizable strong phase, which plays an essential role in accommodating the observed CP violation. The second is that a large value of $\rho_A > 2$ is required, echoing the previous results reported in Refs. [35,111–114]. Such a large ρ_A poses a substantial challenge to the QCDF

approach, as it places considerable strain on the validity of the power counting scheme.

The resulting branching ratios and CP asymmetries, calculated using the S1 optimal parameters, are presented in Table VII. The columns labeled "a_i", "$a_{i,I}^p$", "a_i^p" correspond to the results obtained in the NF scheme with the coefficient a_i in Eq. (25), and in the QCDF approach with the coefficients "$a_{i,I}^p$" and "a_i^p" in Eq. (27), respectively, excluding and including the HSS contributions. The columns labeled "$a_i + b_i$" and "$a_i^p + b_i$" denote the results obtained with the WA amplitudes $\mathcal{M}_{\pi\pi}^a$ included. The PDG data are also provided for comparison. It is clearly seen that the WA contributions have a great impact on the branching ratio for the $B \to \pi^0\pi^0$ decay.

The χ_i distributions [see Eq. (36)], which illustrate the discrepancies between the theoretical expectations and the experimental measurements, are displayed in Fig. 3, with the uncertainties propagated from the fitted parameters. As can be seen from Fig. 3, the primary discrepancies between the theoretical expectations and the PDG data originate from the branching ratios, in addition to the direct CP asymmetry $\mathcal{C}_{CP}(\pi^0\pi^0)$. This tension cannot be easily reconciled without going beyond the conventional QCDF framework and introducing additional contributions, for instance, the soft COME contributions that will be elaborated on in the following discussion.

TABLE VI. Best-fit parameters and their correlations for Scenario S1.

	Value	Correlation matrix		
$\chi^2/n_{\rm dof}$	52.2/4	$F_0^{B\pi}$	ρ_A	ϕ_A
$F_0^{B\pi}$	0.251 ± 0.004	1.00	0.01	−0.18
ρ_A	2.30 ± 0.07		1.00	0.19
ϕ_A	$(162.3 \pm 1.4)°$			1.00

B. Scenario S2

The constraints on the free parameters in Scenario S2 are derived primarily from branching ratios rather than from CP asymmetries, as shown in Fig. 4. As is evident from

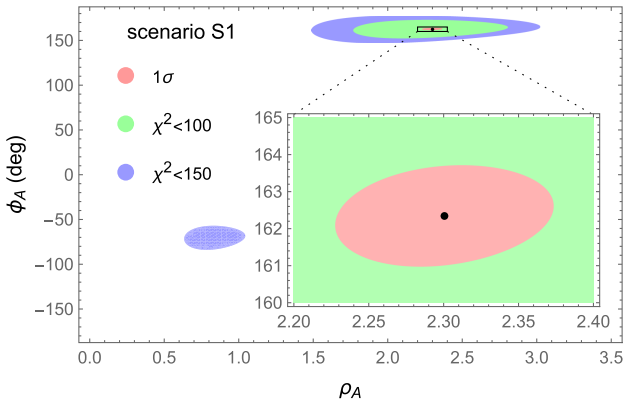


FIG. 2. Optimal parameters for Scenario S1 obtained from the PDG data. In the inset, the oval represents the 1σ region of the fitted parameters, and the dot denotes the best-fit result.

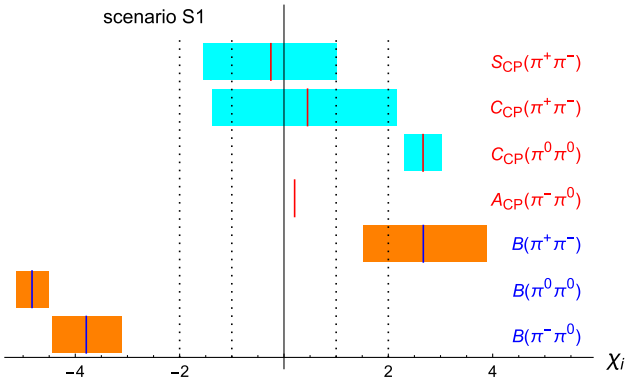


FIG. 3. χ_i distributions with the optimal S1 parameters. The vertical bars and horizontal bands correspond to the central values and uncertainties of the respective observables, respectively.

TABLE VII. Branching ratios and CP asymmetries for the $B \to \pi\pi$ decays with the S1 optimal parameters. The theoretical uncertainties are derived from the errors of the fitted parameters. See the text for the definitions of the columns.

	a_i	$a_{i,I}^p$	a_i^p	$a_i + b_i$	$a_i^p + b_i$	PDG
$10^6 \times \mathcal{B}(\pi^-\pi^0)$	5.15	4.15	4.32	5.15	4.32 ± 0.17	5.31 ± 0.26
$10^6 \times \mathcal{B}(\pi^+\pi^-)$	7.11	7.87	7.69	5.61	$6.12^{+0.32}_{-0.30}$	5.43 ± 0.26
$10^6 \times \mathcal{B}(\pi^0\pi^0)$	0.20	0.18	0.17	0.70	0.54 ± 0.06	1.46 ± 0.19
$\mathcal{A}_{CP}(\pi^-\pi^0)$		−0.004	−0.002		-0.002 ± 0.000	-0.01 ± 0.04
$\mathcal{C}_{CP}(\pi^+\pi^-)$		0.043	0.048	−0.375	$-0.300^{+0.051}_{-0.055}$	-0.314 ± 0.030
$\mathcal{S}_{CP}(\pi^+\pi^-)$	−0.420	−0.495	−0.496	−0.592	$-0.678^{+0.038}_{-0.039}$	-0.67 ± 0.03
$\mathcal{C}_{CP}(\pi^0\pi^0)$		−0.440	0.021	0.442	$0.250^{+0.064}_{-0.066}$	-0.23 ± 0.18
$\mathcal{S}_{CP}(\pi^0\pi^0)$	0.994	0.116	0.473	0.884	$0.880^{+0.031}_{-0.036}$	

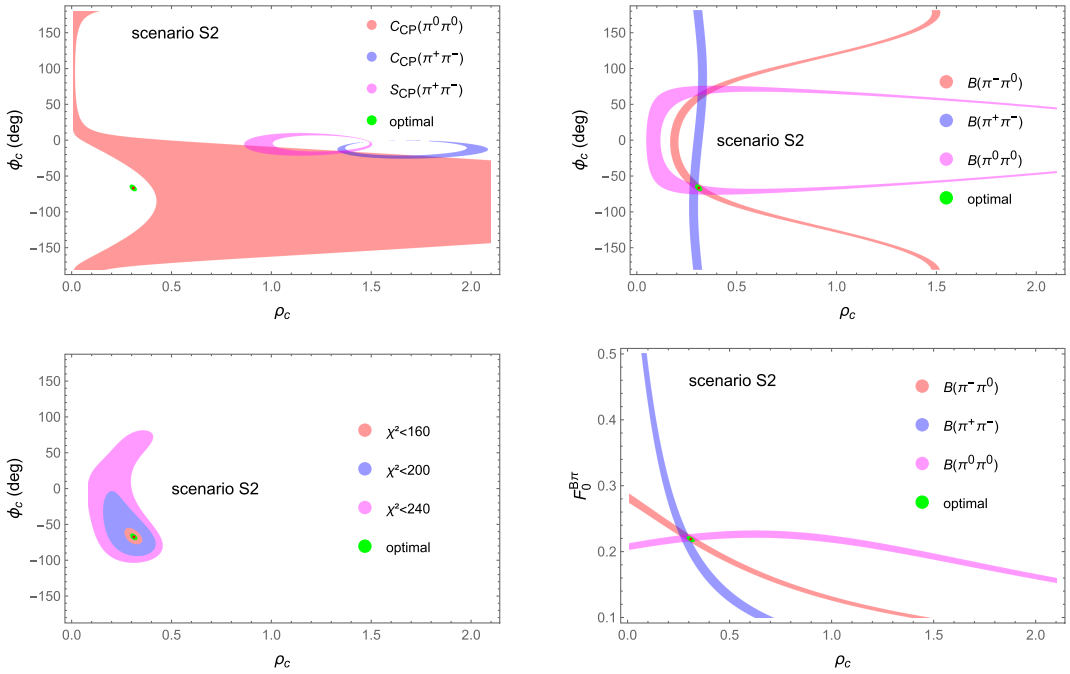


FIG. 4. Constraints on the S2 parameters. Other legends are the same as those of Fig. 1.

the distribution in the (ρ_c, ϕ_c) plane, the simultaneous crossing region of the CP asymmetry bands, located near the point $(1.36, -17°)$, is far away from the best-fit region. This situation is physically unacceptable and indicates that the resulting fits cannot provide a consistent and physically reasonable interpretation of the CP asymmetry measurements.

TABLE VIII. Best-fit parameters and their correlations for Scenario S2.

	Value	Correlation matrix		
$\chi^2/n_{\rm dof}$	154.1/4	$F_0^{B\pi}$	ρ_c	ϕ_c
$F_0^{B\pi}$	0.220 ± 0.005	1.00	−0.59	0.23
ρ_c	0.31 ± 0.02		1.00	−0.49
ϕ_c	$(-66.6 \pm 4.8)°$			1.00

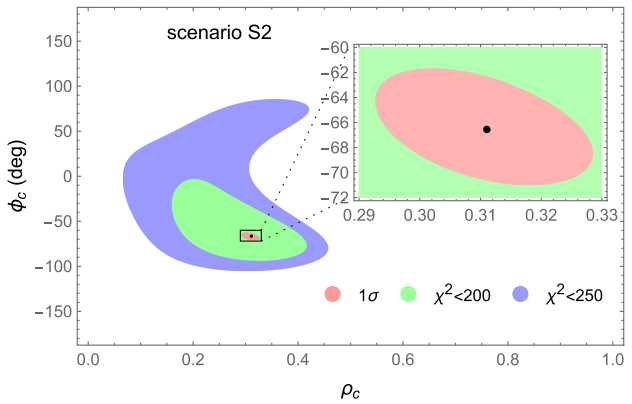


FIG. 5. Optimal parameters for Scenario S2 obtained from the PDG data. The inset shares the same legend as Fig. 2.

The optimal values of the free parameters obtained with the PDG data for Scenario S2 are shown in Table VIII. The best-fit values of the soft COME parameters ρ_c and ϕ_c are illustrated in Fig. 5. Scenario S2 exhibits two distinctive features. First, the form factor $F_0^{B\pi}$ in Scenario S2 is slightly smaller than its counterpart in Scenario S1. This reduction can be largely attributed to the inclusion of soft COME contributions in Scenario S2. Second, the parameter ρ_c is found to be around 0.3, suggesting that the soft COME contributions do not play a dominant role. Furthermore, the value of ρ_c is comparable to that[1] obtained in the PQCD approach, where the contributions from the HSS and WA amplitudes are taken into account along with a larger form factor $F_0^{B\pi} = 0.27$ [41].

The resulting branching ratios and CP asymmetries, calculated using the S2 optimal values of parameters, are presented in Table IX. The columns labeled "a_i", "$a_{i,I}^p$" correspond to the results obtained in the NF scheme with the coefficient a_i in Eq. (25) and in the QCDF approach with the coefficient "$a_{i,I}^p$" in Eq. (27) excluding the HSS contributions, respectively. The columns labeled "$a_i + c_i$" and "$a_{i,I}^p + c_i$" denote the results obtained with the soft COME amplitudes $\mathcal{M}_{\pi\pi}^c$ included. It is clearly seen that soft

[1] ρ_c corresponds to the parameter d_1 of Eq. (71) in Ref. [41]. It should be noted that the two parameters ρ_c and d_1 are defined within different factorization frameworks and should not be directly identified.

TABLE IX. Branching ratios and CP asymmetries for the $B \to \pi\pi$ decays with the S2 optimal parameters. Other legends are the same as those of Table VII.

	a_i	$a_{i,I}^p$	$a_i + c_i$	$a_{i,I}^p + c_i$	PDG
$10^6 \times \mathcal{B}(\pi^-\pi^0)$	3.97	3.20	6.04	$5.29^{+0.54}_{-0.50}$	5.31 ± 0.26
$10^6 \times \mathcal{B}(\pi^+\pi^-)$	5.48	6.06	4.80	5.33 ± 0.44	5.43 ± 0.26
$10^6 \times \mathcal{B}(\pi^0\pi^0)$	0.16	0.14	1.76	$1.67^{+0.29}_{-0.26}$	1.46 ± 0.19
$\mathcal{A}_{CP}(\pi^-\pi^0)$		−0.004	0.003	−0.002	-0.01 ± 0.04
$\mathcal{C}_{CP}(\pi^+\pi^-)$		0.043	−0.012	0.016 ± 0.003	-0.314 ± 0.030
$\mathcal{S}_{CP}(\pi^+\pi^-)$	−0.420	−0.495	−0.422	-0.509 ± 0.003	-0.67 ± 0.03
$\mathcal{C}_{CP}(\pi^0\pi^0)$		−0.440	−0.353	-0.512 ± 0.040	-0.23 ± 0.18
$\mathcal{S}_{CP}(\pi^0\pi^0)$	0.994	0.116	0.066	$-0.003^{+0.054}_{-0.049}$	

COME contributions are remarkably significant for the branching ratio of the $B \to \pi^0\pi^0$ decay, whereas their impact on the $B \to \pi^+\pi^-$ decay is marginal.

The χ_i distributions are displayed in Fig. 6. It is evident that the primary discrepancies originate from the CP asymmetries $\mathcal{C}_{CP}(\pi^+\pi^-)$ and $\mathcal{S}_{CP}(\pi^+\pi^-)$, owing to the absence of the potential strong phases associated with the WA contributions.

C. Scenario S3

The constraints on the free parameters in Scenario S3 are illustrated in Fig. 7. Scenario S3 incorporates more free parameters, thereby substantially enhancing the flexibility and effective dimensionality of the parameter space. In Figs. 1 and 4, the parameter regions permitted by the branching ratio constraints do not overlap with those allowed by the CP asymmetry constraints. In Fig. 7, these previously incompatible regions are found to intersect, indicating that the internal tensions among the constraints are largely alleviated and that the overall compatibility with observational data is markedly improved.

The optimal values of the free parameters obtained from fits to the PDG data for Scenario S3 are summarized in Table X. The best-fit values of the parameters are illustrated in Fig. 8. Scenario S3 exhibits several distinctive features: (1) The goodness-of-fit, $\chi^2/n_{\rm dof}$, is better in Scenario S3 than in Scenarios S1 and S2; (2) Owing to the inclusion of both the WA and soft COME contributions, the form factor $F_0^{B\pi}$ in Scenario S3 is smaller than its counterparts in Scenarios S1 and S2, and also smaller than the typical values adopted in earlier QCDF and PQCD analyses [30–35,41,42]. This value is compatible, within the quoted uncertainties, with the recent lattice QCD determination, $F_0^{B\pi} = 0.183(92)$ [116], as well as with the recent light-cone sum rule result, $F_0^{B\pi} = 0.19(5)$ [117]; (3) The WA parameter ρ_A is found to be less than 1. This result is consistent with the QCDF conjecture on the strength of WA effects and simultaneously underscores the importance of soft COME contributions; (4) The value of the soft COME parameter ρ_c in Scenario S3 is slightly smaller than its counterpart in Scenario S2, further reinforcing the importance of WA amplitudes. The negative correlation between ρ_c and ϕ_c is consistent with the pattern found in Scenario S2, suggesting that the soft COME parameter space is already well-constrained by the branching ratio data; (5) Owing to the increased number of free parameters in Scenario S3, the constraining power of the fit on individual parameters is correspondingly weakened, leading to larger uncertainties for ϕ_A and ϕ_c compared with their counterparts in Scenarios S1 and S2, respectively. The increased uncertainties for ϕ_A and ϕ_c in Scenario S3 reflect the limited constraining power of the current experimental data. This indicates that, while the combined scenario provides a better overall fit, some parameter combinations remain loosely constrained. Future measurements with improved precision will be essential for further pinning down these parameters and for testing the viability of Scenario S3.

The resulting branching ratios and CP asymmetries, calculated using the Scenario S3 optimal values of parameters, are presented in Table XI. The columns labeled "a_i", "a_i^p" correspond to the results obtained in the NF scheme

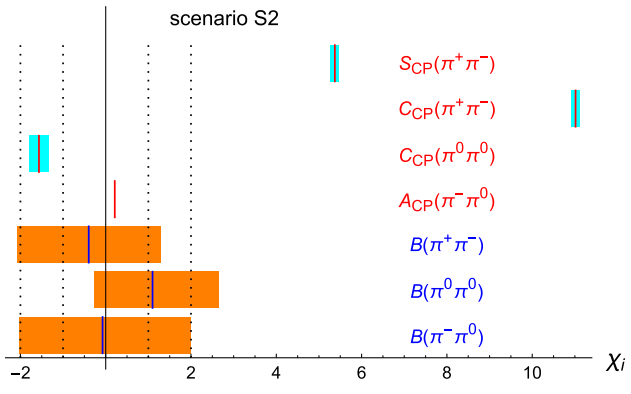


FIG. 6. χ_i distributions for the optimal S2 parameters. Other legends are the same as those of Fig. 3.

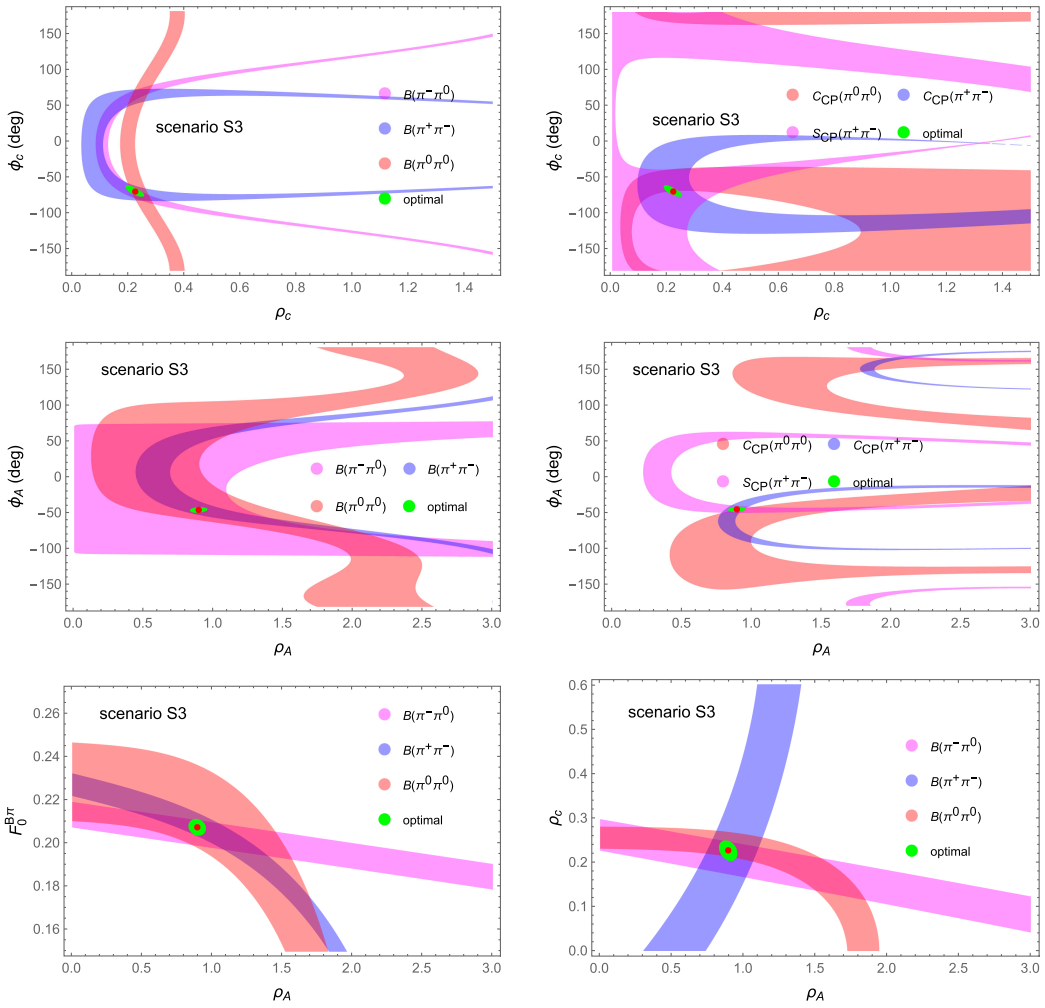


FIG. 7. Constraints on the S3 parameters. Other legends are the same as those of Fig. 1.

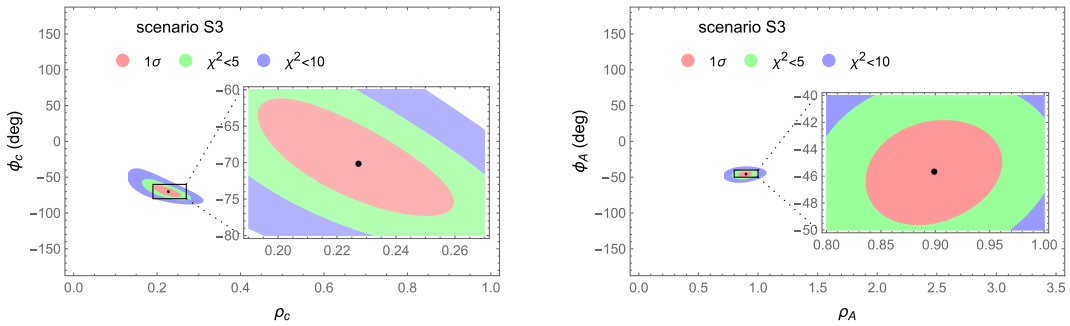


FIG. 8. Optimal parameters for Scenario S3 obtained from the PDG data. The inset shares the same legend as Fig. 2.

TABLE X. Best-fit parameters and their correlations for Scenario S3.

	Value	Correlation matrix				
$\chi^2/n_{\rm dof}$	1.73/2	$F_0^{B\pi}$	ρ_c	ϕ_c	ρ_A	ϕ_A
$F_0^{B\pi}$	0.207 ± 0.005	1.00	−0.42	0.19	−0.07	−0.44
ρ_c	0.23 ± 0.04		1.00	−0.77	−0.33	0.13
ϕ_c	$(-70.2 \pm 8.4)°$			1.00	0.28	0.04
ρ_A	0.90 ± 0.07				1.00	0.21
ϕ_A	$(-45.7 \pm 4.4)°$					1.00

TABLE XI. Branching ratios and CP asymmetries for the $B \to \pi\pi$ decays with the S3 optimal parameters. Other legends are the same as those of Table VII.

	a_i	a_i^p	$a_i^p + c_i$	$a_i^p + b_i$	$a_i^p + b_i + c_i$	PDG
$10^6 \times \mathcal{B}(\pi^-\pi^0)$	3.52	4.10	5.42	4.10	$5.42^{+0.37}_{-0.40}$	5.31 ± 0.26
$10^6 \times \mathcal{B}(\pi^+\pi^-)$	4.86	4.32	3.98	5.94	$5.36^{+0.40}_{-0.38}$	5.43 ± 0.26
$10^6 \times \mathcal{B}(\pi^0\pi^0)$	0.14	0.40	1.57	0.51	$1.36^{+0.27}_{-0.24}$	1.46 ± 0.19
$\mathcal{A}_{CP}(\pi^-\pi^0)$		−0.005	−0.001	−0.005	-0.001 ± 0.001	-0.01 ± 0.04
$\mathcal{C}_{CP}(\pi^+\pi^-)$		0.043	0.017	−0.255	$-0.321^{+0.042}_{-0.044}$	-0.314 ± 0.030
$\mathcal{S}_{CP}(\pi^+\pi^-)$	−0.420	−0.518	−0.528	−0.696	$-0.671^{+0.041}_{-0.044}$	-0.67 ± 0.03
$\mathcal{C}_{CP}(\pi^0\pi^0)$		−0.372	−0.440	0.296	$-0.417^{+0.186}_{-0.150}$	-0.23 ± 0.18
$\mathcal{S}_{CP}(\pi^0\pi^0)$	0.994	0.766	0.150	0.830	$0.735^{+0.142}_{-0.167}$	

with the coefficient a_i in Eq. (25) and in the QCDF approach with the coefficient "a_i^p" in Eq. (27) including the HSS contributions, respectively. The columns labeled "$a_i^p + c_i$" and "$a_i^p + b_i$" denote the results obtained with the soft COME amplitudes $\mathcal{M}^c_{\pi\pi}$ and the WA amplitudes $\mathcal{M}^a_{\pi\pi}$ included, respectively. The columns labeled "$a_i^p + b_i + c_i$" denote the preferred results obtained with amplitudes in Eq. (35). It is clearly seen that soft COME contributions significantly enhance the branching ratio of the color-suppressed $B \to \pi^0\pi^0$ decay, and that the WA contributions play a very important role in the branching ratio of the color-allowed $B \to \pi^+\pi^-$ decay. More importantly, for the vast majority of observables, including branching ratios and CP asymmetries, the Scenario S3 results (the "$a_i^p + b_i + c_i$" column) are found to be consistent with the corresponding experimental measurements within the quoted uncertainties. This overall agreement is further corroborated by the χ_i distributions shown in Fig. 9, which demonstrate that Scenario S3 provides a satisfactory description of the data for virtually all $B \to \pi\pi$ decay modes. This consistency may offer a possible resolution to the so-called "$\pi\pi$ puzzle".

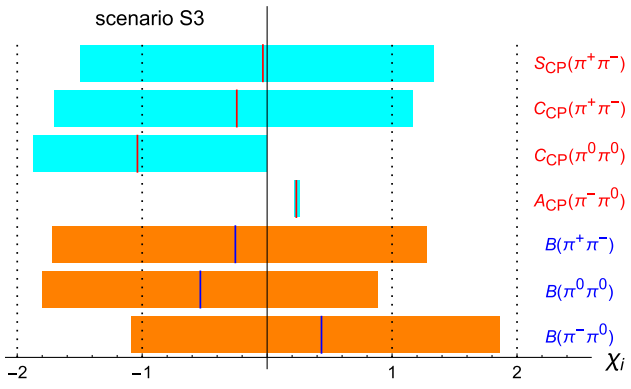


FIG. 9. χ_i distributions for the optimal S3 parameters. Other legends are the same as those of Fig. 3.

IV. SUMMARY

In this paper, we have revisited the $B \to \pi\pi$ decays within the QCDF framework, with particular emphasis on the role of soft COME contributions that are usually neglected in the conventional QCDF approach. Our primary goal has been to investigate whether the inclusion of these soft nonperturbative effects can offer a resolution to the long-standing "$\pi\pi$ puzzle".

We have formulated three distinct phenomenological scenarios for the fits. Scenario S1, which corresponds to the conventional QCDF prescription and includes the WA contributions, reproduces the previous finding that a large WA parameter, $\rho_A > 2$, is required to accommodate the experimental data. Such a large value, however, places considerable strain on the validity of the power counting scheme. Scenario S2, which includes soft COME contributions, yields a phenomenologically consistent value of $\rho_c \sim 0.3$, in agreement with the PQCD expectation, but fails to account for the observed CP asymmetries because the WA-induced strong phases are absent. The combined scenario, Scenario S3, which incorporates both the WA and soft COME amplitudes, provides an excellent overall description of almost all observables. The goodness-of-fit for the PDG data is significantly improved compared with Scenarios S1 and S2, and the theoretical and experimental branching ratios and CP asymmetries fall within the quoted uncertainties. Moreover, the fitted WA parameter in Scenario S3 satisfies $\rho_A < 1$, which is consistent with the QCDF expectation that WA contributions are power suppressed.

From the numerical analysis, we draw the following conclusions: (1) The soft COME contributions play a particularly significant role in the color-suppressed $B \to \pi^0\pi^0$ decay; (2) The WA contributions are essential for generating the necessary strong phases to describe the CP asymmetries; (3) Only when both types of contributions are included simultaneously can the QCDF framework accommodate almost all $B \to \pi\pi$ observables in a theoretically consistent and empirically satisfactory manner.

In summary, our results indicate that soft COME contributions, overlooked in the conventional QCDF treatment, may serve as a crucial ingredient for resolving the "$\pi\pi$ puzzle". The soft COME amplitudes naturally explain the observed hierarchy among the branching ratios without invoking unnaturally large WA parameters. This work therefore provides a possible way to reconcile the long-standing discrepancies between theory and experiment within the SM, and calls for further theoretical scrutiny of soft COME contributions from first-principles QCD calculations. Future high-precision measurements will be essential for further testing the scenario proposed in this work.

ACKNOWLEDGMENTS

This work is supported by the National Natural Science Foundation of China (Grant No. 12275068), the National Key R&D Program of China (Grant No. 2023YFA1606000), and the Natural Science Foundation of Henan Province (Grant No. 262300421308, No. 252300421491).

DATA AVAILABILITY

There are no publicly available research data or software supporting this manuscript. Requests for further information or data should be sent to the authors.

[1] F. Takahashi, K. Hikasa, Y. Sumino *et al.* (Particle Data Group), Review of particle physics, Int. J. Mod. Phys. A **41**, 2630011 (2026).
[2] C. Dib, I. Dunietz, F. Gilman, and Y. Nir, Standard-model predictions for CP violation in B^0-meson decay, Phys. Rev. D **41**, 1522 (1990).
[3] M. Gronau and D. London, Isospin analysis of CP asymmetries in B decays, Phys. Rev. Lett. **65**, 3381 (1990).
[4] H. Lipkin, Y. Nir, H. Quinn, and A. Snyder, Penguin trapping with isospin analysis and CP asymmetries in B decays, Phys. Rev. D **44**, 1454 (1991).
[5] N. Cabibbo, Unitary symmetry and leptonic decays, Phys. Rev. Lett. **10**, 531 (1963).
[6] M. Kobayashi and T. Maskawa, CP-violation in the renormalizable theory of weak interaction, Prog. Theor. Phys. **49**, 652 (1973).
[7] M. Beneke, G. Buchalla, M. Neubert, and C. Sachrajda, QCD factorization for $B \to \pi\pi$ decays: Strong phases and CP violation in the heavy quark limit, Phys. Rev. Lett. **83**, 1914 (1999).
[8] M. Beneke, G. Buchalla, M. Neubert, and C. Sachrajda, QCD factorization for exclusive nonleptonic B meson decays: General arguments and the case of heavy light final states, Nucl. Phys. **B591**, 313 (2000).
[9] D. Du, D. Yang, and G. Zhu, Analysis of the decays $B \to \pi\pi$ and πK with QCD factorization in the heavy quark limit, Phys. Lett. B **488**, 46 (2000).
[10] D. Du, D. Yang, and G. Zhu, Infrared divergence and twist-3 distribution amplitudes in QCD factorization for $B \to PP$, Phys. Lett. B **509**, 263 (2001).
[11] D. Du, D. Yang, and G. Zhu, QCD factorization for $B \to PP$, Phys. Rev. D **64**, 014036 (2001).
[12] M. Beneke, G. Buchalla, M. Neubert, and C. Sachrajda, QCD factorization in $B \to \pi K, \pi\pi$ decays and extraction of Wolfenstein parameters, Nucl. Phys. **B606**, 245 (2001).
[13] H. Li and H. Yu, Extraction of V_{ub} from the decay $B \to \pi\ell\nu$, Phys. Rev. Lett. **74**, 4388 (1995).
[14] H. Li, Study of the decay $B \to \pi\pi$ via perturbative QCD, Phys. Lett. B **348**, 597 (1995).
[15] Y. Keum, H. Li, and A. Sanda, Fat penguins and imaginary penguins in perturbative QCD, Phys. Lett. B **504**, 6 (2001).
[16] Y. Keum, H. Li, and A. Sanda, Penguin enhancement and $B \to K\pi$ decays in perturbative QCD, Phys. Rev. D **63**, 054008 (2001).
[17] Y. Keum and H. Li, Nonleptonic charmless B decays: Factorization versus perturbative QCD, Phys. Rev. D **63**, 074006 (2001).
[18] C. Lü, K. Ukai, and M. Yang, Branching ratio and CP violation of $B \to \pi\pi$ decays in the perturbative QCD approach, Phys. Rev. D **63**, 074009 (2001).
[19] C. Lü and M. Yang, $B \to \pi\rho, \pi\omega$ decays in perturbative QCD approach, Eur. Phys. J. C **23**, 275 (2002).
[20] H. Li and K. Ukai, Threshold resummation for nonleptonic B meson decays, Phys. Lett. B **555**, 197 (2003).
[21] Y. Duh, T. Wu, P. Chang *et al.* (Belle Collaboration), Measurements of branching fractions and direct CP asymmetries for $B \to K\pi$, $B \to \pi\pi$ and $B \to KK$ decays, Phys. Rev. D **87**, 031103 (2013).
[22] B. Aubert, M. Bona, D. Boutigny *et al.* (*BABAR* Collaboration), Study of $B^0 \to \pi^0\pi^0$, $B^\pm \to \pi^\pm\pi^0$, and $B^\pm \to K^\pm\pi^0$ decays, and isospin analysis of $B \to \pi\pi$ decays, Phys. Rev. D **76**, 091102 (2007).
[23] I. Adachi, L. Aggarwal, H. Ahmed *et al.* (Belle II Collaboration), Measurement of branching fractions and direct CP asymmetries for $B \to K\pi$ and $B \to \pi\pi$ decays at Belle II, Phys. Rev. D **109**, 012001 (2024).
[24] T. Julius, M. Sevior, G. Mohanty *et al.* (Belle Collaboration), Measurement of the branching fraction and CP asymmetry in $B^0 \to \pi^0\pi^0$ decays, and an improved constraint on ϕ_2, Phys. Rev. D **96**, 032007 (2017).
[25] J. Lees, V. Poireau, V. Tisserand *et al.* (*BABAR* Collaboration), Measurement of CP asymmetries and branching fractions in charmless two-body B-meson decays to pions and kaons, Phys. Rev. D **87**, 052009 (2013).
[26] I. Adachi, L. Aggarwal, H. Ahmed *et al.* (Belle II Collaboration), Measurement of the branching fraction and CP-violating asymmetry of the decay $B^0 \to \pi^0\pi^0$

using 387 million $\Upsilon(4S)$ decays in Belle II data, Phys. Rev. D **111**, L071102 (2025).
[27] B. Aubert, R. Barate, M. Bona *et al.* (*BABAR* Collaboration), Improved measurements of the branching fractions for $B^0 \to \pi^+\pi^-$ and $B^0 \to K^+\pi^-$, and a search for $B^0 \to K^+K^-$, Phys. Rev. D **75**, 012008 (2007).
[28] M. Abumusabh, I. Adachi, K. Adamczyk *et al.* (Belle II Collaboration), Measurement of mixing-induced CP violating in the decay $B^0 \to \pi^0\pi^0$, arXiv:2606.20797.
[29] J. Dalseno, K. Prothmann, C. Kiesling *et al.* (Belle Collaboration), Measurement of the CP violation parameters in $B^0 \to \pi^+\pi^-$ decays, Phys. Rev. D **88**, 092003 (2013).
[30] D. Du, H. Gong, J. Sun, D. Yang, and G. Zhu, Phenomenological analysis of $B \to PP$ decays with QCD factorization, Phys. Rev. D **65**, 074001 (2002).
[31] M. Beneke and M. Neubert, QCD factorization for $B \to PP$ and $B \to PV$ decays, Nucl. Phys. **B675**, 333 (2003).
[32] M. Beneke, T. Huber, and X. Li, NNLO vertex corrections to non-leptonic B decays: Tree amplitudes, Nucl. Phys. **B832**, 109 (2010).
[33] C. Qiao, R. Zhu, X. Wu, and S. Brodsky, A possible solution to the $B \to \pi\pi$ puzzle using the principle of maximum conformality, Phys. Lett. B **748**, 422 (2015).
[34] H. Cheng and C. Chua, Revisiting charmless hadronic $B_{u,d}$ decays in QCD factorization, Phys. Rev. D **80**, 114008 (2009).
[35] Q. Chang, J. Sun, Y. Yang, and X. Li, Spectator scattering and annihilation contributions as a solution to the πK and $\pi\pi$ puzzles within QCD factorization approach, Phys. Rev. D **90**, 054019 (2014).
[36] A. Williamson and J. Zupan, Two body B decays with isosinglet final states in soft collinear effective theory, Phys. Rev. D **74**, 014003 (2006); Phys. Rev. D **74**, 039901 (E) (2006).
[37] Y. Zhang, X. Liu, Y. Fan, S. Cheng, and Z. Xiao, $B \to \pi\pi$ decays and effects of the next-to-leading order contributions, Phys. Rev. D **90**, 014029 (2014).
[38] X. Liu, H. Li, and Z. Xiao, Transverse-momentum-dependent wave functions with Glauber gluons in $B \to \pi\pi$, $\rho\rho$ decays, Phys. Rev. D **91**, 114019 (2015).
[39] Y. Yang, L. Lang, X. Zhao, J. Huang, and J. Sun, Reinvestigating the $B \to PP$ decays by including the contributions from ϕ_{B2}, Phys. Rev. D **103**, 056006 (2021).
[40] J. Chai, S. Cheng, Y. Ju, D. Yan, C. Lü, and Z. Xiao, Charmless two-body B meson decays in the perturbative QCD factorization approach, Chin. Phys. C **46**, 123103 (2022).
[41] S. Lü and M. Yang, Possible solution of the puzzle for the branching ratio and CP violation in $B \to \pi\pi$ decays with a modified perturbative QCD approach, Phys. Rev. D **107**, 013004 (2023).
[42] S. Lü, R. Wang, and M. Yang, Study of $B \to PP$ decays in the modified perturbative QCD approach, Phys. Rev. D **110**, 056025 (2024).
[43] R. Wang and M. Yang, Branching ratio and CP violation of $B \to K\pi$ decays in a modified perturbative QCD approach, Phys. Rev. D **108**, 013003 (2023).
[44] Y. Gui and M. Yang, Study of $B \to \rho\eta$, $\rho\eta'$ decays in the modified perturbative QCD approach, Phys. Rev. D **111**, 036007 (2025).
[45] R. Wang and M. Yang, Revisiting $B \to K^*\pi$ and $B \to K\rho$ decays using the modified perturbative QCD approach, Eur. Phys. J. C **85**, 146 (2025).
[46] S. Lü and M. Yang, Study of $B \to \pi\rho$, $\pi\omega$ decays in the modified perturbative QCD approach, Eur. Phys. J. C **85**, 821 (2025).
[47] R. Wang and M. Yang, Branching fraction, CP asymmetry, and polarization in $B \to \rho\rho$ decays with the modified perturbative QCD approach, J. Phys. G **52**, 105001 (2025).
[48] G. Altarelli and L. Maiani, Octet enhancement of non-leptonic weak interactions in asymptotically free gauge theories, Phys. Lett. **52B**, 351 (1974).
[49] H. Fritzsch, How to discover the B mesons, Phys. Lett. **86B**, 343 (1979).
[50] N. Deshpande, M. Gronau, and D. Sutherland, Final state gluon effects in charmed meson decays, Phys. Lett. **90B**, 431 (1980).
[51] Y. Igarashi, S. Kitakado, and M. Kuroda, Soft hadron interaction effects in charmed meson decays, Phys. Lett. **93B**, 125 (1980).
[52] H. Fritzsch and P. Minkowski, Tests of the quark annihilation hypothesis for D and F decays, Nucl. Phys. **B171**, 413 (1980).
[53] J. Finjord, The magnitude of annihilation and penguin contributions to charm meson decays, Nucl. Phys. **B181**, 74 (1981); Nucl. Phys. **B198**, 544(E) (1982).
[54] M. Gronau and D. Sutherland, Soft gluonic effects in non-leptonic decays, Nucl. Phys. **B183**, 367 (1981).
[55] Q. Ho-Kim and H. Lee, Gluon effects in charmed meson decays, Phys. Lett. **100B**, 420 (1981).
[56] J. Finjord, Decays of charmed mesons via color octet decays of the c-quark, Phys. Lett. **109B**, 227 (1982).
[57] Q. Ho-Kim and H. Lee, Decays of charmed mesons, Phys. Rev. D **25**, 178 (1982).
[58] A. Buras, J. Gérard, and R. Rückl, $1/N_c$ expansion for exclusive and inclusive charm decays, Nucl. Phys. **B268**, 16 (1986).
[59] H. Cheng, Vacuum insertion and nonperturbative effects for exclusive nonleptonic decays of charmed mesons and kaons, Z. Phys. C **32**, 237 (1986).
[60] H. Cheng, Status of the $\Delta I = \frac{1}{2}$ rule in kaon decay, Int. J. Mod. Phys. A **04**, 495 (1989).
[61] A. Deandrea, N. Bartolomeo, R. Gatto, and G. Nardulli, Two-body nonleptonic decays of B and B_s mesons, Phys. Lett. B **318**, 549 (1993).
[62] B. Blok and M. Shifman, Nonfactorizable amplitudes in weak nonleptonic decays of heavy mesons, Nucl. Phys. **B389**, 534 (1993).
[63] B. Blok and M. Shifman, The rule of discarding $1/N_c$ in inclusive weak decays (I), Nucl. Phys. **B399**, 441 (1993).
[64] H. Cheng, Nonfactorizable contributions to nonleptonic weak decays of heavy mesons, Phys. Lett. B **335**, 428 (1994).
[65] I. Halperin, Soft gluon suppression of $1/N_c$ contributions in color suppressed heavy meson decays, Phys. Lett. B **349**, 548 (1995).

[66] J. Soares, "Nonfactorizable" terms in hadronic B-meson weak decays, Phys. Rev. D **51**, 3518 (1995).
[67] H. Cheng and B. Tseng, Extraction of a_1 and a_2 from $B \to \psi K(K^*)$, $D(D^*)\pi(\rho)$ decays, Phys. Rev. D **51**, 6259 (1995).
[68] A. Kamal, A. Santra, T. Uppal, and R. Verma, Nonfactorization in hadronic two-body Cabibbo favored decays of D^0 and D^+, Phys. Rev. D **53**, 2506 (1996).
[69] R. Verma, Searching a systematics for nonfactorizable contributions to hadronic decays of D^0 and D^+ mesons, Z. Phys. C **69**, 253 (1996).
[70] H. Cheng, Hadronic weak decays of heavy mesons and nonfactorization, Z. Phys. C **69**, 647 (1996).
[71] A. Kamal and A. Santra, Nonfactorization and the decays $D_s^+ \to \phi\pi^+$, $\phi\rho^+$, and $\phi\ell^+\nu_\ell$, Z. Phys. C **71**, 101 (1996).
[72] A. Kamal and A. Santra, Nonfactorization and color-suppressed $B \to \psi(\psi') + K(K^*)$ decays, Z. Phys. C **72**, 91 (1996).
[73] J. Donoghue and A. Petrov, Factorization in nonleptonic decays of heavy mesons, Phys. Lett. B **393**, 149 (1997).
[74] H. Cheng, Can $B \to J/\psi K(K^*)$ decays be described by factorization?, Phys. Lett. B **395**, 345 (1997).
[75] A. Katoch and K. Sharma, Nonfactorizable contributions to hadronic decays of charm mesons in the Cabibbo-suppressed modes, Z. Phys. C **75**, 651 (1997).
[76] K. Sharma, A. Katoch, and R. Verma, Nonfactorizable contributions to charm meson ($D \to PP$) decays, Z. Phys. C **76**, 311 (1997).
[77] A. Katoch, K. Sharma, and R. Verma, Isospin analysis of non-factorizable contributions to hadronic decays of charm mesons, J. Phys. G **23**, 807 (1997).
[78] F. Al-Shamali and A. Kamal, Nonfactorization and final state interactions in $(B, B_s) \to \psi P$ and ψV decays, Eur. Phys. J. C **4**, 669 (1998).
[79] H. Cheng and B. Tseng, Nonfactorizable effects in spectator and penguin amplitudes of hadronic charmless B decays, Phys. Rev. D **58**, 094005 (1998).
[80] M. Neubert and B. Stech, Nonleptonic weak decays of B mesons, Adv. Ser. Dir. High Energy Phys. **15**, 294 (1998).
[81] F. Al-Shamali and A. Kamal, Nonfactorization in Cabibbo favored B decays, Phys. Rev. D **59**, 054020 (1999).
[82] K. Sharma and A. Katoch, An isospin analysis of non-factorizable contributions to hadronic decays of bottom mesons, Mod. Phys. Lett. A **14**, 1841 (1999).
[83] Y. Chen, H. Cheng, and B. Tseng, Charmless hadronic two-body decays of B_s mesons, Phys. Rev. D **59**, 074003 (1999).
[84] H. Cheng and K. Yang, Updated analysis of a_1 and a_2 in hadronic two-body decays of B mesons, Phys. Rev. D **59**, 092004 (1999).
[85] F. Al-Shamali and A. Kamal, Factorization and nonfactorization in B decays, Phys. Rev. D **60**, 114019 (1999).
[86] A. Khodjamirian, $B \to \pi\pi$ decay in QCD, Nucl. Phys. **B605**, 558 (2001).
[87] A. Khodjamirian, Th. Mannel, and B. Melić, QCD light-cone sum rule estimate of charming penguin contributions in $B \to \pi\pi$, Phys. Lett. B **571**, 75 (2003).
[88] S. Mantry, D. Pirjol, and I. Stewart, Strong phases and factorization for color suppressed decays, Phys. Rev. D **68**, 114009 (2003).
[89] A. Khodjamirian, Th. Mannel, M. Melcher, and B. Melić, Annihilation effects in $B \to \pi\pi$ from QCD light-cone sum rules, Phys. Rev. D **72**, 094012 (2005).
[90] R. Dhir and R. Verma, Nonfactorizable contributions to hadronic decays of D mesons, J. Phys. G **34**, 637 (2007).
[91] X. Wu, B. Zhang, H. Li, X. Liu, B. Liu, J. Li, and Y. Guo, Non-factorization contributions in $D \to \pi K$, KK decay, Phys. Lett. B **675**, 196 (2009).
[92] M. Kaur, S. Singh, and R. Verma, Searching systematics for nonfactorizable contributions to B^- and $\bar{B}^0$ hadronic decays, Chin. Phys. C **46**, 073105 (2022).
[93] M. Piscopo and A. Rusov, Non-factorisable effects in the decays $\bar{B}_s^0 \to D_s^+\pi^-$ and $\bar{B}^0 \to D^+K^-$ from LCSR, J. High Energy Phys. 10 (2023) 180.
[94] M. Kaur, S. Singh, and R. Verma, p-wave mesons emitting weak decays of bottom mesons, Chin. Phys. C **49**, 023105 (2025).
[95] G. Buchalla, A. Buras, and M. Lautenbacher, Weak decays beyond leading logarithms, Rev. Mod. Phys. **68**, 1125 (1996).
[96] L. Wolfenstein, Parametrization of the Kobayashi-Maskawa Matrix, Phys. Rev. Lett. **51**, 1945 (1983).
[97] A. Buras, M. Lautenbacher, and G. Ostermaier, Waiting for the top quark mass, $K^+ \to \pi^+\nu\bar{\nu}$, $B_s^0 - \bar{B}_s^0$ mixing, and CP asymmetries in B decays, Phys. Rev. D **50**, 3433 (1994).
[98] P. Ball, V. Braun, and A. Lenz, Higher-twist distribution amplitudes of the K meson in QCD, J. High Energy Phys. 05 (2006) 004.
[99] O. Haan and B. Stech, Violation of the $\Delta I = 1/2$ rule in non-leptonic decays, Nucl. Phys. **B22**, 448 (1970).
[100] M. Gaillard, B. Lee, and J. Rosner, Search for charm, Rev. Mod. Phys. **47**, 277 (1975).
[101] J. Ellis, M. Gaillard, and D. Nanopoulos, On the weak decays of high mass hadrons, Nucl. Phys. **B100**, 313 (1975); Nucl. Phys. **B104**, 547(E) (1976).
[102] D. Fakirov and B. Stech, F and D decays, Nucl. Phys. **B133**, 315 (1978).
[103] V. Chernyak and A. Zhitnitsky, Exclusive decays of heavy mesons, Nucl. Phys. **B201**, 492 (1982); Nucl. Phys. **B214**, 547(E) (1983).
[104] A. Buras and J. Gérard, $1/N$ expansion for kaons, Nucl. Phys. **B264**, 371 (1986).
[105] M. Bauer, B. Stech, and M. Wirbel, Exclusive nonleptonic decays of D-, D_s-, and B mesons, Z. Phys. C **34**, 103 (1987).
[106] J. Bjorken, Topics in B-physics, Nucl. Phys. B, Proc. Suppl. **11**, 325 (1989).
[107] M. Wirbel, B. Stech, and M Bauer, Exclusive semileptonic decays of heavy mesons, Z. Phys. C **29**, 637 (1985).
[108] H. Fritzsch and P. Minkowski, The puzzle of nonleptonic decays and its resolution, Phys. Lett. **90B**, 455 (1980).
[109] G. Lepage and S. Brodsky, Exclusive processes in perturbative quantum chromodynamics, Phys. Rev. D **22**, 2157 (1980).
[110] G. Bell, M. Beneke, T. Huber, and X. Li, Two-loop nonleptonic penguin amplitude in QCD factorization, J. High Energy Phys. 04 (2020) 055.
[111] Q. Chang, J. Sun, Y. Yang, and X. Li, A combined fit on the annihilation corrections in $B_{u,d,s} \to PP$ decays within QCDF, Phys. Lett. B **740**, 56 (2015).

[112] J. Sun, Q. Chang, X. Hu, and Y. Yang, Constraints on hard spectator scattering and annihilation corrections in $B_{u,d} \to PV$ decays within QCD factorization, Phys. Lett. B **743**, 444 (2015).

[113] Q. Chang, X. Hu, J. Sun, and Y. Yang, Probing spectator scattering and annihilation corrections in $B_s \to PV$ decays, Phys. Rev. D **91**, 074026 (2015).

[114] Q. Chang, X. Li, J. Sun, and Y. Yang, Fits of weak annihilation and hard spectator scattering corrections in $B_{u,d} \to VV$ decays, J. Phys. G **43**, 105004 (2016).

[115] K. Wang and G. Zhu, Flavor dependence of annihilation parameters in QCD factorization, Phys. Rev. D **88**, 014043 (2013).

[116] B. Colquhoun, S. Hashimoto, T. Kaneko, and J. Koponen (JLQCD Collaboration), Form factors of $B \to \pi\ell\nu$ and a determination of $|V_{ub}|$ with Möbius domain-wall fermions, Phys. Rev. D **106**, 054502 (2022).

[117] B. Cui, Y. Huang, Y. Shen, C. Wang, and Y. Wang, Precision calculations of $B_{d,s} \to \pi, K$ decay form factors in soft-collinear effective theory, J. High Energy Phys. 03 (2023) 140.